



# Hydrological impacts of future climate and land use/cover changes in the Lower Mekong Basin: a case study of the Srepok River Basin, Vietnam

Pham Thi Thao Nhi · Dao Nguyen Khoi ·  
Nguyen Thi Thuy Trang · Tran Van Ty ·  
Shibo Fang

Received: 9 December 2020 / Accepted: 10 September 2021

© The Author(s), under exclusive licence to Springer Nature Switzerland AG 2022

**Abstract** This study presents hydrological impacts of future climate change (CC) and land use/cover change (LUCC) for the Srepok River Basin (SRB) in the Vietnam's Central Highlands. The hydrology cycle of this basin was reproduced using Soil and Water Assessment Tool (SWAT) allowing an evaluation of hydrological responses to CC and LUCC. Future climate scenarios of the 2015–2100 period under Representative Concentration Pathways (RCP) 4.5 simulated by five General Circulation Models (GCMs) and LUCC scenario in

2050 were developed. Compared to the reference scenario (1980–2005), future LUCC increases the streamflow (0.25%) and surface runoff (1.2%) and reduces the groundwater discharge (2.1%). Climate change may cause upward trends in streamflow (0.1 to 2.7%), surface runoff (0.4 to 4.3%), and evapotranspiration (0.8 to 3%), and a change in the groundwater discharge (−1.7 to 0.1%). The combination of CC and LUCC increases the streamflow (0.2 to 2.8%), surface runoff (1.6 to 5.6%), and evapotranspiration (1.0 to 3.1%), and reduces the groundwater discharge (1.5 to 2.7%) with respect to the reference scenario. Moreover, the results noted that the water scarcity may happen in the dry-seasonal months.

Topical Collection on *Environmental sustainability and impacts of climate change in the Mekong delta region*

P. T. T. Nhi · D. N. Khoi (✉) · N. T. T. Trang  
Faculty of Environment, University of Science, 227  
Nguyen Van Cu Str., Dist. 5, Ho Chi Minh City, Vietnam  
e-mail: dnkhoi@hcmus.edu.vn; dnkhoi86@gmail.com

P. T. T. Nhi · D. N. Khoi · N. T. T. Trang  
Vietnam National University Ho Chi Minh City, Linh  
Trung Ward, Thu Duc Dist, Ho Chi Minh City, Vietnam

P. T. T. Nhi  
Institute for Computational Science and Technology,  
Ho Chi Minh City 700000, Vietnam

T. Van Ty  
College of Technology, Can Tho University, Ninh Kieu  
Dist, Campus 2, 3/2 Str, Can Tho City, Vietnam

S. Fang  
Institution of Ecological and Agricultural Meteorology,  
Chinese Academy of Meteorological Sciences,  
Beijing 100081, People's Republic of China

**Keywords** Climate change · Hydrology · Land use/cover change · Srepok River Basin · SWAT model

## Introduction

In recent years, freshwater resources are under serious pressure as a consequence of the effects of climate change (CC), land use/cover change (LUCC) (Abera et al., 2019), continued population growth, and socio-economic development (IPCC, 2013). Freshwater resources assessment has become a difficult task because many factors must be considered, and CC and LUCC are two decisive and important environmental factors influencing catchment hydrology (Zhang et al., 2016). Many studies have indicated that temperature rise and rainfall change alter spatio-temporal patterns

of hydrological regimes, including evapotranspiration, infiltration, surface runoff, lateral flow, and base flow, and accordingly influence characteristics of freshwater resources (Azmat et al., 2018), while LUCC attributable to human activities can result in changes of the regional hydrological processes, including infiltration, surface runoff, and groundwater (Woldesenbet et al., 2017). Therefore, in order to support water management under a changing environment, the effects of CC and LUCC on freshwater resources needs to be quantified.

There are various studies on examining the CC and LUCC impacts on hydrological components and water availability at regional scale, such as Thailand (Shrestha et al., 2018), Indonesia (Setyorini et al., 2017), China (Bao et al., 2019; Han et al., 2019), Malaysia (Tan et al., 2015), Italy (Napoli et al., 2017), Australia (Cheng & Yu, 2019), and the USA (Hung et al., 2020). Broadly speaking, the approaches of inspecting the CC and LUCC impacts on hydrological components comprise comparison of paired basins, statistical method in reliance on analyzing the hydro-meteorological data, and hydrological simulation (Chen et al., 2020). In the midst of these approaches, the hydrological simulation was selected for the study by a reason of its advantage in scenario studies regarding the interconnections between climate, land use/cover, and hydrology.

There are several hydrological models applied to hydrological studies under the CC and LUC impacts, including the Hydrological Engineering Center's-Hydrological Modeling System (HEC-HMS), Hydrological Simulation Program-Fortran (HSPF), MIKE-Systeme Hydrologique European (MIKE-SHE), and Soil and Water Assessment Tool (SWAT). Amidst these hydrological models, the SWAT model has been extensively used in hydrological investigations under the environmental changes because it has proved to be as an effective tool for hydrological simulation in many basins around the globe (e.g., Fan & Shibata, 2015; Hung et al., 2020; Osei et al., 2019; Shrestha et al., 2018). The approaches used to produce future climate scenarios based on General Circulation Model (GCM) outputs are divided into statistical and dynamical downscaling techniques. The dynamical downscaling technique necessitates running a higher-resolution Regional Climate Model (RCM) on regional sub-domain within a coarser-resolution GCM. Compared to dynamical downscaling technique,

statistical technique is easily applied to different areas at the station scale and requires insignificant computing resources (Wilby & Dawson, 2007). Among statistical downscaling tools, the Long Ashton Research Stochastic Weather Generator (LARS-WG) is one of the most widely used tools for studies on CC impact (e.g., Allani et al., 2020; Kavwenje et al., 2021; Qin & Lu, 2014). Moreover, LARS-WG has a strong capacity to retain key statistical properties of weather events compared to other statistical methods, such as the Weather Generator (WGEN) and Statistical Downscaling Model (SDSM) (Qin & Lu, 2014). Regarding projections of LUCC, the methods vary from generalized assumptions of future conversions (Khoi & Suetsugi, 2014; Trang et al., 2017) to LUCC modelling based on the historical trends and driving factors of LUCC (El-Khoury et al., 2015). Among the land use/cover projection methods, the modeling approach is preferred owing to the fact that it can produce realistic projections of LUCC (El-Khoury et al., 2015).

Changes in streamflow and hydrological components could be of the importance for large basins, such as the Srepok River Basin (SRB), which is one of major tributaries of the Lower Mekong River Basin. The SRB has economic significance to Vietnam with a substantial contribution of agricultural production (coffee, pepper, and rubber). Nevertheless, this basin has experienced alterations in climate and LUCC over recent years. Specifically, the SRB had suffered deforestation with a rate of 0.31%/year attributable to an extension of perennial crops in recent years and population growth in the 2000–2010 period (Meyfroidt et al., 2013). Moreover, the climate of the SRB had become hotter and wetter with a 0.4 °C rise in temperature and a 9.2% rise in rainfall during the 1980–2010 period (Khoi & Thom, 2015a, b). Regarding this issue, there are a few studies on the CC and LUCC impacts on hydrology conducted in Vietnam. As an example, Khoi and Suetsugi (2014) analyzed the CC and LUCC impacts on hydrological processes in the Be River Basin, and they found that CC is the major cause of changes in catchment hydrology. In that study, the LUCC scenarios are simple. They were built based on historical trends of LUCC in the study area, without considering factors affecting LUCs (e.g., land-use policy and socioeconomic conditions). Additionally, Zhang et al. (2016) demonstrated that the hydrological impacts of CC and LUCC vary from place to place and it is essential to examine at local scales.

This study aimed to estimate the separate and integrated impacts of future CC and LUCC on stream-flow and hydrological components in the SRB located in Vietnam’s Central Highlands. This study devotes important guiding information that required by decision-makers in the field of sustainable management of water resources.

**Study area**

The SRB, a sub-basin of the Mekong River Basin, located in Vietnam’s Central Highlands has an area of approximately 12,000 km<sup>2</sup> (Fig. 1). The Srepok River with the length of about 291 km is formed by two main tributaries, namely, the Krong No River and Krong Ana River. The average altitude of the SRB varies between 100 m and 2,400 m in the northwest-southeast direction. The climate in the basin is tropical monsoon with high humidity of 78–83% and annual rainfall of 1,700–2,300 mm, and it is separated into two seasons: a dry season (November to April) and a wet season (May to October). The annual flow is approximately 300 m<sup>3</sup>/s and the peak flow often

occur in October. The SRB has abundant freshwater resources and aquatic biodiversity, which have supported the livelihoods of approximately 2.4 million people in 2014. Furthermore, the main soil type of this basin is basaltic soil, which is the beneficial condition for agricultural development. Productions of perennial crops, including coffee and rubber, are strength of this region in exporting agricultural products in Vietnam.

**Methodology**

**Hydrological simulation**

The SWAT model is a basin scale, semi-distributed, time-continuous, and process-based model, which is developed by the Agricultural Research Service of the US Department of Agriculture (USDA) (Neitsch et al., 2011). This model is designed to model hydrological processes, soil erosion, and water quality in large agricultural basin. In SWAT, the hydrological cycle is simulated at each hydrological response unit (HRU) using the balance equation of soil water as follows

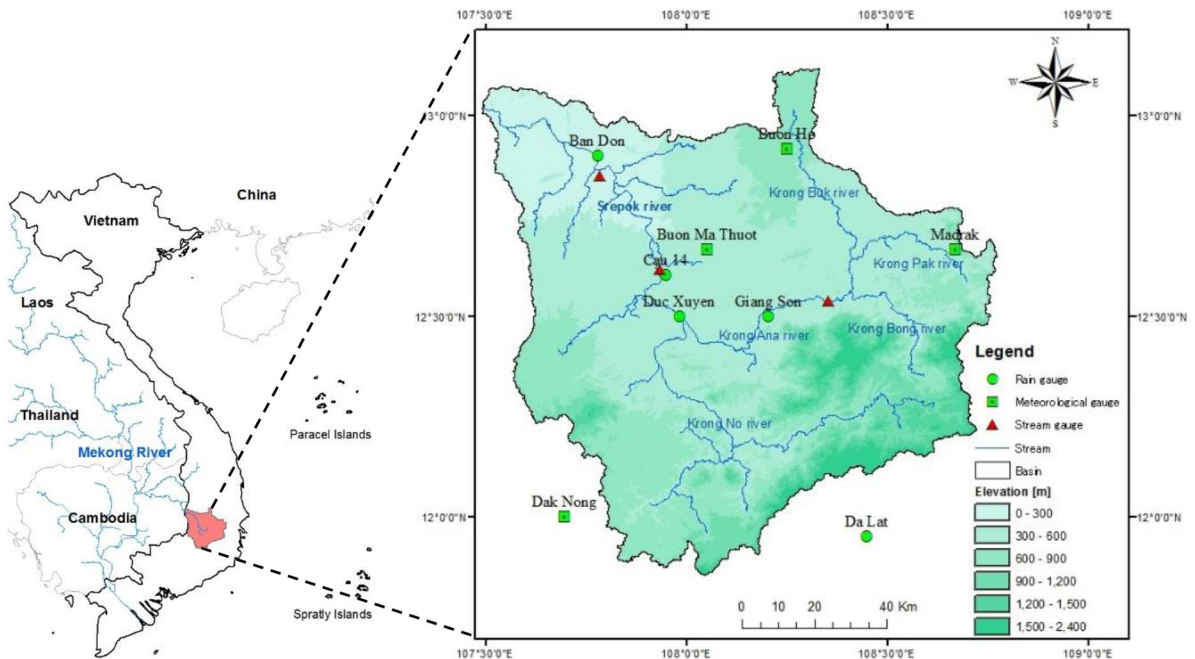


**Fig. 1** The SRB and location of hydro-meteorological stations

$$SW_t = SW_0 + \sum_{i=1}^t (R_{\text{day}} - Q_{\text{surf}} - E_e - w_{\text{seep}} - Q_{\text{gw}})$$

where  $SW_t$  is the final soil water content (mm),  $SW_0$  is the initial soil water content (mm),  $t$  is the time (days),  $R_{\text{day}}$  is the precipitation (mm),  $Q_{\text{surf}}$  is the surface runoff (mm),  $E_e$  is the evapotranspiration (mm),  $w_{\text{seep}}$  is the water entering the vadose zone from the soil profile (mm), and  $Q_{\text{gw}}$  is the return flow or groundwater flow (mm).

In the present study, the Penman–Monteith procedure was utilized for estimating the potential and actual evapotranspiration. The hydrological processes in reliance on surface runoff generation and channel routing were estimated using the Soil Conservation Service–Curve Number (SCS-CN) and variable storage approaches. Further details related to the SWAT model can be found in the reference of Neitsch et al. (2011).

In the present study, SWAT 2012 with an interface supported by ArcGIS Desktop 10.3 developed by ESRI was employed. The SWAT requires spatial and temporal data as listed in Table 1 to simulate the catchment hydrology. After the data were prepared, the model setup was performed the following main steps:

In the first step, the SWAT used the 90 m DEM for basin configuration and topographical parameterization. The SRB was delineated and subdivided into 72 sub-basins with a threshold area of 8,000 ha and the characteristics of the basin, such as slope gradient, slope length, and the streamflow network characteristics were also generated. In the second step, the HRU definition was performed through the “HRU analysis” module. Based on unique land-use type, soil type, and slope class, the sub-basins have been further divided into HRUs with the threshold value of 10% for land-use, slope, and soil. Overall, there were 930 HRUs defined in the entire basin within 72 sub-basins. The third step is to run using the necessary meteorological data inputs and the essential information from

HRUs defined from the previous step. Then, the rain gauges and the weather stations were assigned to each sub-basins based on their proximity to centroids of the sub-basins. The simulation was run first for the reference period of 1980 to 2005 using the first year as a warm-up period to stabilize the model. In the last step in the modelling process, the SWAT model was calibrated with 10 years of discharge data (1981–1990) and validated with 15 years of discharge data (1991–2005) at the three hydrological stations, namely Giang Son, Cau 14, and Ban Don, using the Sequential Uncertainty Fitting version 2 (SUFI-2) method, which is implemented in SWAT-CUP 2012 (Abbaspour, 2015). The SUFI-2 is the adequate technique for calibration and validation of the SWAT model in the tropical regions (Khoi & Thom, 2015a, b; Khoi et al., 2017).

The model evaluation with observed streamflow data, graphical comparison (i.e., line and column charts), and statistical analyses was used. The graphical method is used to illustrate the qualitative relationship between measured and simulated values. As for the statistical analysis, three statistical indices used include the Nash–Sutcliffe efficiency (NS), percent bias (PBIAS), and the ratio of root mean square error (RMSE) to the standard deviation (STD) of measured data (RSR). A positive PBIAS value indicates model underestimations and a negative PBIAS value indicates model overestimations. The model performance for flow simulations is satisfactory when NS values greater than 0.5, PBIAS values less than 15%, and RSR values less than 0.7 (Moriassi et al., 2015).

### Scenarios of climate change

The LARS-WG is a stochastic weather generator, it was used to project future climatic conditions (i.e., precipitation and temperature) in this work. This model uses

**Table 1** Data sources for the SRB

Data type	Data description	Scale	Data sources
Terrain	Digital elevation model	90 m	US Geological Survey (USGS)
Land-use	Land use/cover classification such as agricultural land, forest, and urban	1 km	Mekong River Commission (MRC)
Soil	Soil classification and physical properties	10 km	Food and Agriculture Organization (FAO)
Meteorology	Daily precipitation, minimum and maximum temperature	Daily	Hydro-Meteorological Data Centre (HMDC)

the observed daily climate data to calculate a set of parameters for semi-empirical probability distributions of weather variables (daily precipitation, minimum and maximum temperature), which were then used to generate weather time series of arbitrary length by randomly selecting values from the appropriate distribution (Chen et al., 2013). The detail of the LARS-WG methodology was discussed by Semenov and Stratonovitch (2010). For the statistical analysis of the observed and generated data, the performance of LARG-WG was evaluated. The performance of the LARS-WG for simulating the observed climate data was assessed by using the coefficient of correlation ( $R^2$ ) and root mean squared error (RMSE). The two statistical indices have been widely used to assess the performance of statistical downscaling tools in simulating the climate variables (e.g., Agarwal et al., 2014; Hassan et al., 2014).

To generate future climate scenarios for our study area, the distribution parameters for a given site were perturbed by the predicted climate using the GCM output. The RCP4.5 emission scenario was used for projecting the future climate for three periods: near-term period of 2020s (2015–2040), mid-term period of 2050s (2045–2070), and long-term period of 2080s (2075–2100) based on an average ensemble of 5 GCM outputs incorporated in LARS-WG (Table 2). Use of the GCM ensemble will minimize the potential bias of any specific GCM and helps to better estimate the projected uncertainties (Knutti et al., 2010). The RCP4.5 was selected for the present study because it projects a future with a balanced emphasis on all energy sources and it is the most popularly scenario in the IPCC—Fifth Assessment Report (AR5) (IPCC, 2013). In addition, differences in future precipitation and temperature between greenhouse gas (GHG) emission scenarios are small and the importance of using multi-GCMs in assessing the CC impact on hydrology is highlighted (Hoan et al., 2020; Khoi & Suetsugi, 2012).

### Scenarios of Land use/cover

The land use/cover maps used in this work were collected from the study of Ty et al. (2012). In that study, a simple geographic information system (GIS)-based logistic regression approach was used to predict future LUCC. First, the available land use/cover types were reclassified into five main groups: thick forestland, thin forestland, grassland, agricultural land, and urban land. The relationship between each land use/cover type and its driving factors (e.g., population, agro-climatic conditions, and socio-economic development) was then determined using logistic regression, and probability maps of each land use/cover type were produced, accordingly. To predict future land use/cover types in 2050, the population density in 2050 was considered as the driving factor on land use/cover change. Based on that, the probability maps were updated new values of the driving factor (Ty et al., 2012).

The land use/cover types in 1997 and the predicted land use/cover types 2050 are displayed in Fig. 2. The figure indicates the expansion of agricultural land, urban area, and grassland. For the entire basin, the agricultural land, urban land, and grassland are predicted to increase from 28.5 to 32.6%, 0.1 to 5.7%, and 36.8 to 43.9% between 1997 and 2050, respectively. In contrast, the forestland is likely to reduce from 29.6% in 1997 to 15.6% in 2050.

## Results and discussion

### Simulation performance of the SWAT model

In the present study, sensitivity analysis was performed to identify key hydrological parameters influencing the water cycle in the SWAT model using the SUFI-2.

**Table 2** Five GCMs from IPCC-AR5 incorporated in LAR-WG

Center, country	Model identifier	Grid resolution
National Oceanic and Atmospheric Administration (NOAA), Geophysical Fluid Dynamics Laboratory, USA	EC-EARTH	1.1215 × 1.125°
European Centre for Medium-Range Weather Forecasts, Europe	GFDL-CM3	2 × 2.5°
UK Met. Office, UK	HadGEM2-ES	1.25 × 1.875°
Meteorological Research Institute, Japan	MIROC5	1.4008 × 1.40625°
Max-Planck Institute for Meteorology, Germany	MPI-ESM-MR	1.8653 × 1.875°

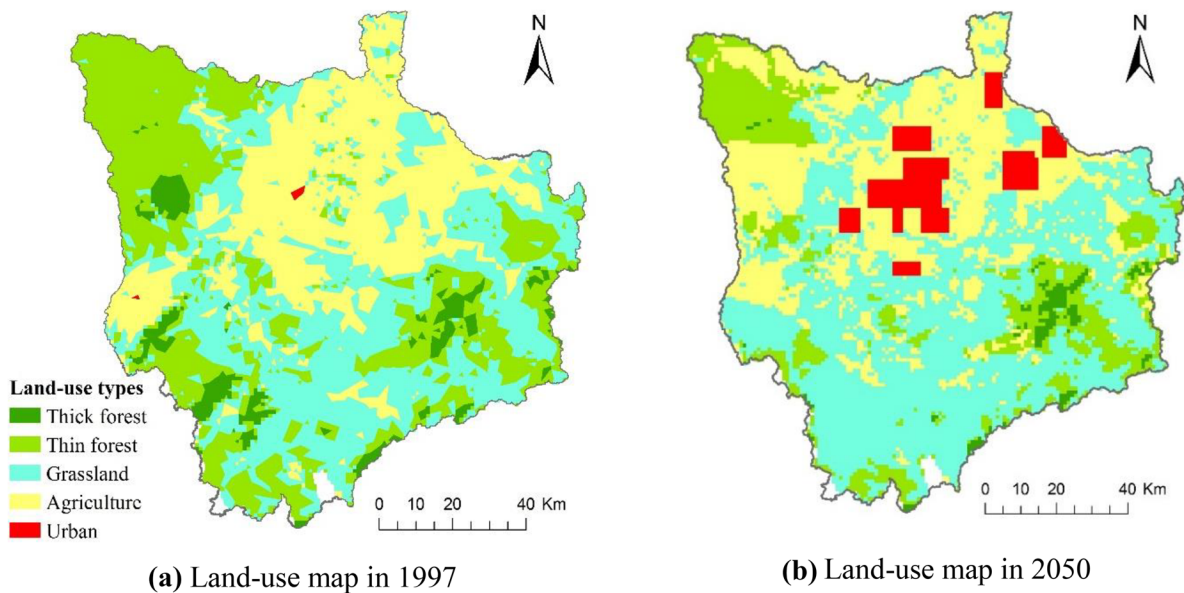


**Fig. 2** Land-use maps in **a** 1997 and **b** 2050

Table 3 displays 26 hydrological parameters with their *t*-value and *p*-value statistics which represent their relative sensitivities. Based on the result of sensitivity analysis (Table 3), five key parameters controlling the SRB's hydrological processes, including the curve number (CN2), the channel effective hydraulic conductivity (CH\_K2), the baseflow alpha factor (ALPHA\_BF), the available water capacity (SOL\_AWC), and Manning's value for the main channel (CH\_N2), were identified and used for calibration and validation of the SWAT model. Table 4 lists their calibrated values.

The SWAT calibration and validation for daily streamflow were conducted at three main gauging stations (the Giang Son, Cau 14, and Ban Don stations) in the SRB. As depicted in Fig. 3, the model could generate similar trends between the observed and simulated daily streamflow during both the calibration (1981–1990) and validation (1991–2005) periods. In spite of the fact that the similar trends were obtained, some peak discharge and low flow events were not consistent, which may be associated to the uneven spatial distribution of weather stations. An additional reason comes from the CN2 method, which is used to simulate surface runoff. The CN2 values are calculated as a function of land use/cover feature, soil feature, and hydrological conditions, which was produced by studies involving relationships between rainfall and

runoff from agricultural catchments across the USA (Neitsch et al., 2011). In actuality, this method has given good performances when applied in the USA. However, this may not true when applied in the Vietnam's tropical climate. Based on the statistical analyses of the SWAT performance on a daily time-scale (Table 5), the measured and simulated streamflow were strongly consistent with the NS, PBIAS and RSR values, which varied in the range of 0.64 to 0.71, –15 to –10%, and 0.53 to 0.59 in the calibration period, respectively. Regarding the validation period, the NS, PBIAS, and RSR values varied from 0.65 to 0.78, –14 to –1%, and 0.46 to 0.59, respectively.

Using aggregated monthly average streamflow values based on daily streamflow values increased the agreement between the simulated and observed values. This agreement was indicated by the NS, PBIAS, and RSR values, which ranged from 0.70 to 0.86, –15 to –10%, and 0.37 to 0.55 for the calibration period; and 0.81 to 0.85, –14 to –1%, and 0.39 to 0.44 for the validation period, respectively. According to the efficiency criteria given by Moriasi et al. (2015), the NS, PBIAS, and RSR values were rated as good at the Giang Son, Ban Don, and Cau 14 stations in the calibration and validation durations. This suggests that the simulated daily discharge is

**Table 3** Parameter sensitivity analysis for the SWAT in simulating flow

Parameter	Description of parameter	t-value	p-value	Rank
CN2	Initial SCS CN II value	-2.81	0.01	1
CH_K2	Channel effective hydraulic conductivity	2.07	0.05	2
ALPHA_BF	Baseflow alpha factor	-1.89	0.07	3
SOL_AWC	Available water capacity	-1.36	0.19	4
CH_N2	Manning’s n value for main channel	1.35	0.19	5
TLAPS	Temperature lapse rate	0.99	0.33	6
GWQMN	Threshold water depth in the shallow aquifer for flow	0.92	0.37	7
ESCO	Soil evaporation compensation factor	-0.89	0.38	8
SLSUBBSN	Average slope length	-0.72	0.47	9
BIOMIX	Biological mixing efficiency	-0.59	0.56	10
SOL_ALB	Moist soil albedo	0.59	0.56	11
GW_REVAP	Groundwater ‘revap’ coefficient	0.56	0.58	12
HRU_SLP	Average slope steepness	-0.26	0.79	13
REVAPMN	Threshold water depth in the shallow aquifer for “revap”	-0.26	0.80	14
CANMX	Maximum canopy storage	-0.25	0.80	15
GW_DELAY	Groundwater delay	-0.19	0.85	16
EPCO	Plant uptake compensation factor	0.15	0.88	17
SURLAG	Surface runoff lag time	-0.14	0.89	18
BLAI	Maximum potential leaf area index crop	0.14	0.89	19
SOL_K	Saturated hydraulic conductivity	-0.10	0.92	20
SOL_Z	Soil depth	-0.05	0.96	21
SFTMP	Snowfall temperature	-	-	-
SMFMN	Melt factor for snow on December 21 <sup>st</sup>	-	-	-
SMFMX	Melt factor for snow on June 21 <sup>st</sup>	-	-	-
SMTMP	Snow melt base temperature	-	-	-
TIMP	Snow pack temperature lag factor	-	-	-

in good conformity with the measured values. The SWAT performance for this basin is agreed to the previous studies in Vietnam’s Central Highlands conducted by Huyen et al. (2017) and Tram et al. (2019). Overall, the hydrological characteristics of the SRB are well captured using the calibrated and validated SWAT model. Therefore, this model can be applied for further study on hydrological effects of CC and LUCC.

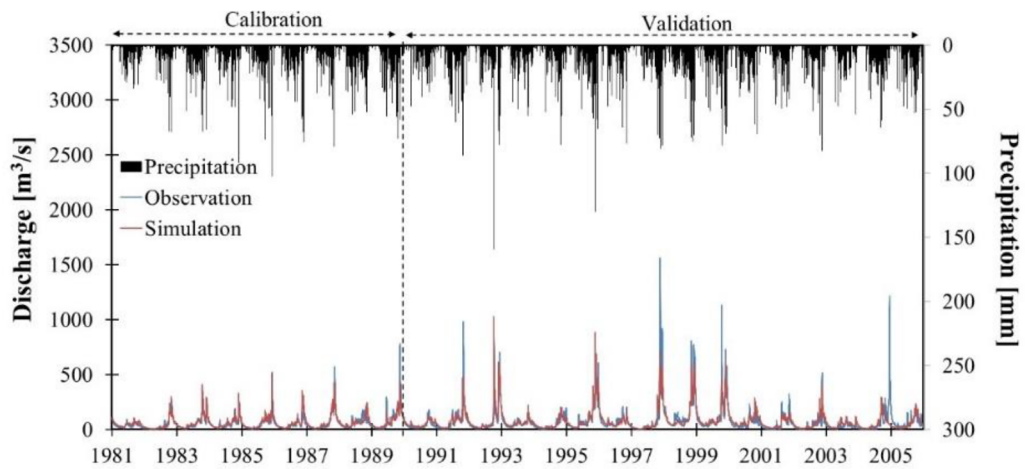
Climate change scenarios

The downscaled daily and monthly rainfall and temperature simulated by LARS-WG during the calibration (1981–1995) and validation (1996–2005) periods are shown in Tables 6 and 7. In the case of rainfall, the differences in the averages of the observed LARS-WG values over all stations were between 0.1 and 0.5 mm/d for daily rainfall and 0.6 and 21.9 mm/

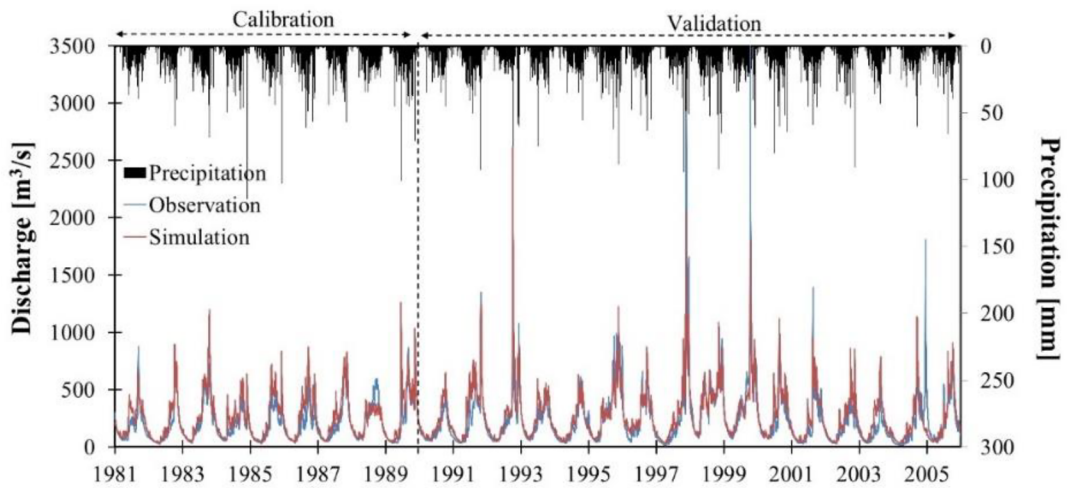
**Table 4** SWAT calibrated values for flow simulation

a parameter value is added by given value, v parameter value is replaced by given value, r parameter value is multiplied by (1 + a given value)

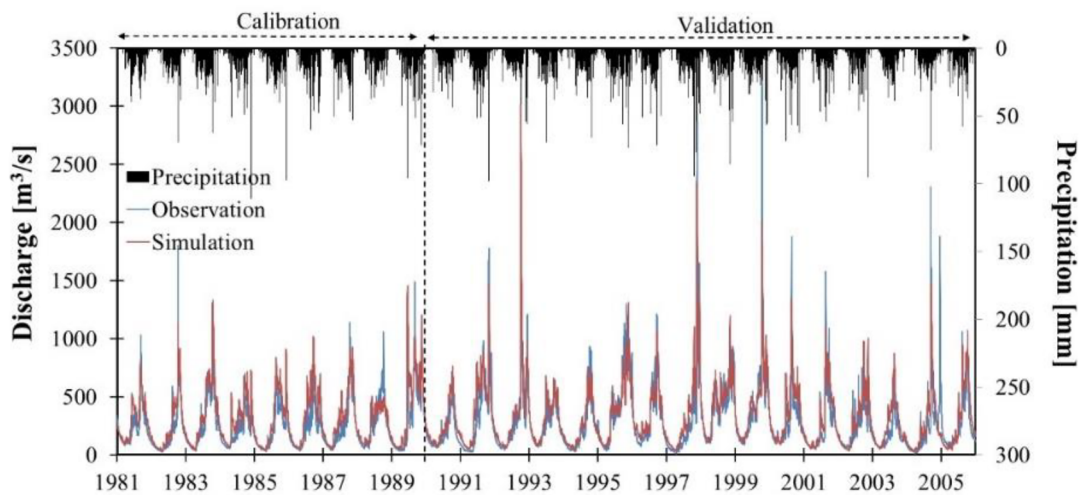
Parameter	Change type	Initial parameter ranges	Best estimation	Final parameter ranges
CN2	r	-0.25 ~ 0.25	-0.17	-0.37 ~ 0.04
CH_K2	a	0 ~ 150	12	-51 ~ 83
ALPHA_BF	v	0 ~ 1	0.11	0 ~ 0.56
SOL_AWC	r	-0.25 ~ 0.25	0.21	-0.01 ~ 0.48
CH_N2	a	0 ~ 1	0.99	0.50 ~ 1.50



(a) Giang Son station



(b) Cau 14 station



(c) Ban Don station



◀ **Fig. 3** Observed and simulated hydrographs at the main hydrological stations during the calibration and validation periods. **a** Giang Son station. **b** Cau 14 station. **c** Ban Don station

month for monthly rainfall. Small differences in the average temperature were recorded by the LARS-WG, and they ranged between 0.1 and 0.5 °C. Regarding the precipitation, the  $R^2$  values ranged from 0.05 to 0.12 for daily simulation and 0.42 to 0.75 for monthly simulation, and the RMSE values varied from 14.7 to 24.2 mm and 95.8 to 211.6 mm for the daily and monthly simulation in the calibration and validation periods, respectively. With regard to  $T_{min}$  and  $T_{max}$ , the  $R^2$  and RMSE values are presented in Table 7. The statistical results of the LARS-WG performance for the SRB were satisfactory and these results are consistent with previous similar studies (i.e., Agarwal et al., 2014; Hassan et al., 2014). In general, downscaling of rainfall is more complex and observed and simulated values are infrequently consistent because of the conditional probability of rainfall events and the intermediate processes of rainfall (fitting probability distribution to observed relative frequencies of wet- and dry-spell lengths) (Hassan et al., 2014). In addition to the statistical assessment, a graphical comparison between the observed and simulated values should be taken into consideration to enhance the confidence of model performance. The comparison plots of observed and simulated average monthly precipitation,  $T_{min}$  and  $T_{max}$  at one station in the upstream part (Dak Nong station) and at another station in the downstream part (Buon Ma Thuot station) of the SRB are presented in Fig. 4. In general term, the LARS-WG was able to satisfactorily reproduce climate features (i.e., precipitation and temperature) of the study area.

Future climate (precipitation and temperature) was generated using the five GCMs driven by the RCP4.5

(Table 2). Figure 5 presents the monthly changes in temperature and precipitation with the uncertainty range of the 5th and 95th percentile bounds for three future periods, including the 2020s (2015 to 2040), 2050s (2045 to 2070), and 2080s (2075 to 2100), with respect to the reference period (1980 to 2005). A general rise in future temperature is observed for all GCMs. The ensemble mean changes in annual temperature are 0.4 °C (within the range of 0.3 to 0.6 °C), 1.1 °C (0.6 to 1.6 °C), and 1.8 °C (1.5 to 2.9 °C) during the 2020s, 2050s, and 2080s, respectively. At a monthly scale, the temperature rises exhibited greater variation and ranged from -0.1 to 0.9 °C, 0.6 to 2.1 °C, and 1.2 to 3.7 °C during the 2020s, 2050s, and 2080s, respectively. Regarding the future precipitation, there is a general increase in annual precipitation. The increases in annual precipitation are 0.4% (within the range of -3.4 to 2.4%), 2.7% (-5.2 to 8.4%), and 2.2% (-5.9 to 9.3%) during the 2020s, 2050s, and 2080s, respectively. The increase in future precipitation is likely attributed to the greenhouse gas (GHG) emission scenarios. In case of seasonality, the dry-seasonal precipitation will significantly reduce within a range from -1.1 to 8.9% and the wet-seasonal precipitation will slightly increase from 0.7 to 5.0%. In general terms, the climate of the SRB is wetter and warmer in the future.

Impact of CC on hydrology

The CC impact on hydrological components is presented in Fig. 6a. Actual evapotranspiration (ET) increases from 0.8 to 3.0%, and potential evapotranspiration (PET) increases by 1.3 to 6.9%. These findings can be justified by rises in future temperature and precipitation. Surface runoff (SURQ), lateral flow (LAT\_Q), and the amount of water percolation (PERC) are expected to have upward trends in the

**Table 5** Model performance for the simulation of streamflow

Station	Time step	Calibration (1981–1990)			Validation (1991–2005)		
		NS	PBIAS	RSR	NS	PBIAS	RSR
Giang Son	Daily	0.71	-10%	0.53	0.65	-1%	0.59
	Monthly	0.86	-10%	0.37	0.81	-1%	0.44
Cau 14	Daily	0.64	-13%	0.59	0.74	-11%	0.51
	Monthly	0.70	-13%	0.55	0.82	-11%	0.42
Ban Don	Daily	0.68	-15%	0.56	0.78	-14%	0.46
	Monthly	0.71	-15%	0.54	0.85	-14%	0.39

**Table 6** The LARS-WG performance in simulation of rainfall

Station	Buon Ma Thuot	Dak Nong	Ban Don	Cau I4	Duc Xuyen	Da Lat	Giang Son	Madrak	Buon Ho			
Calibration (1981–1990)	Daily	Obs (mm)	5.1	4.6	4.4	5.0	5.3	5.0	5.2	5.5	4.2	
		Sim (mm)	5.4	4.4	4.4	5.1	5.4	5.2	5.0	5.0	5.9	4.3
		RMSE (mm)	18.1	18.2	16.0	18.1	16.9	14.7	18.6	18.6	24.2	15.4
	Monthly		$R^2$	0.09	0.07	0.07	0.05	0.11	0.08	0.07	0.06	0.05
			Obs (mm)	156.4	140.6	133.4	150.7	162.3	151.2	158.8	166.2	114.2
			Sim (mm)	162.9	132.2	134.0	155.1	165.7	157.9	153.2	180.8	117.9
			RMSE (mm)	117.1	154.6	101.7	115.0	109.1	108.6	130.0	137.5	100.5
	Validation (1991 – 2000)	Daily	Obs (mm)	0.69	0.63	0.65	0.66	0.72	0.59	0.58	0.69	0.64
			Sim (mm)	5.3	4.7	4.3	4.7	5.1	4.9	5.1	6.0	4.5
			RMSE (mm)	18.4	18.9	14.9	15.6	16.8	14.9	17.5	24.5	16.6
Monthly			$R^2$	0.11	0.07	0.10	0.08	0.12	0.07	0.09	0.06	0.06
			Obs (mm)	160.2	132.6	131.0	142.1	155.5	149.7	154.9	181.7	136.8
			Sim (mm)	159.0	128.0	126.4	137.6	165.3	146.2	158.5	159.8	128.0
			RMSE (mm)	112.1	193.6	93.2	107.2	112.2	95.8	104.0	211.6	119.5
		$R^2$	0.74	0.58	0.72	0.69	0.73	0.64	0.75	0.75	0.42	0.56

**Table 7** The LARS-WG performance in simulation of temperature

Station			Buon Ma Thuot		Dak Nong		Madrak		Buon Ho	
			Tmax	Tmin	Tmax	Tmin	Tmax	Tmin	Tmax	Tmin
Calibration (1981–1990)	Daily	Obs (°C)	29.4	20.5	29.1	18.4	28.8	20.6	26.8	18.7
		Sim (°C)	29.5	20.6	29.1	18.8	28.9	20.8	27.0	19.0
		RMSE (°C)	2.52	1.55	2.71	2.48	3.24	1.83	3.29	2.26
		R <sup>2</sup>	0.57	0.56	0.38	0.54	0.62	0.64	0.48	0.48
	Monthly	Obs (°C)	29.4	20.5	29.1	18.4	28.8	20.6	26.8	18.7
		Sim (°C)	29.5	20.6	29.1	18.8	28.9	20.8	27.0	19.0
		RMSE (°C)	2.56	1.52	2.73	2.45	3.27	1.80	3.31	2.27
		R <sup>2</sup>	0.89	0.89	0.78	0.85	0.93	0.95	0.73	0.73
Validation (1991 – 2000)	Daily	Obs (°C)	29.4	20.7	29.1	19.3	28.8	21.2	27.1	19.3
		Sim (°C)	29.5	20.6	29.0	18.8	28.9	20.8	27.1	19.1
		RMSE (°C)	2.65	1.63	2.70	2.27	3.28	1.81	2.93	2.14
		R <sup>2</sup>	0.52	0.55	0.37	0.58	0.60	0.65	0.51	0.53
	Monthly	Obs (°C)	29.4	20.7	29.1	19.3	28.8	21.2	27.1	19.3
		Sim (°C)	29.5	20.6	29.0	18.8	28.9	20.8	27.1	19.1
		RMSE (°C)	2.62	1.62	2.75	2.26	3.25	1.86	2.94	2.15
		R <sup>2</sup>	0.89	0.92	0.82	0.92	0.93	0.94	0.90	0.85

future by reason of increases in rainfall and evapotranspiration. The increases in SURQ, LAT\_Q, and PERC vary in the range of 0.4 to 4.3%, 0.2 to 1.6%, and 0.0 to 1.0%, respectively. Regarding the other hydrological components, CC will cause a -0.5 to 0.7% change in groundwater discharge (GW\_Q) and a -1.7 to 0.1% change in soil water content (SW). As a general rule, the pattern of change in hydrological components of the SRB is preliminary determined by upward trends in rainfall and temperature.

Figures 6b and 7 illustrate the changes in annual, seasonal, and monthly streamflow with the uncertainty ranges within the 5th and 95th percentile bounds under the CC impact. Comparison of annual streamflow between reference and future climate scenarios, the streamflow is expected to increase by 0.1% (within the range of -6.9 to 5.9%), 2.7% (-14.0% to 17.2%), and 1.7% (-16.4 to 20.3%) during the 2020s, 2050s, and 2080s, respectively. Regarding the seasonal scale, the wet-seasonal streamflow will slightly increase from 0.9 to 5.3% and the dry-seasonal streamflow will reduce from 3.2 to 14.9%. On the whole, the changes in the seasonal streamflow are consistent with changes in the seasonal climate.

### Impact of LUCC on hydrology

The LUCC impact on hydrological components is illustrated in Fig. 8a. Under the LUCC impact, SURQ increases by 1.2%. The GW\_Q and PERC reduce by 2.1 and 2.2%, respectively. However, the other hydrological components (i.e., ET, LAT\_Q, PET, SW, and WYLD) will experience insignificant changes. Deforestation and intensified agricultural expansion could be the cause of these changes because forest vegetation intercepts more water than the other land use/cover types and the infiltration rate of forestland is greater than that of the other land use/cover types (Ma et al., 2009).

Under the LUCC impact, deforestation and agricultural expansion will lead to a slight increase in annual streamflow (0.3%). The upward trend in streamflow is caused by increase in SURQ attributable to deforestation. Considering the seasonal scale, the dry-seasonal streamflow will reduce by 0.2% and the wet-seasonal streamflow will increase by 0.4% (Fig. 8b). The reason that the reduction in dry-seasonal streamflow is likely attributed to changes in evapotranspiration. In the dry season, the precipitation is lower and the temperature is higher than in the wet season (Fig. 5).

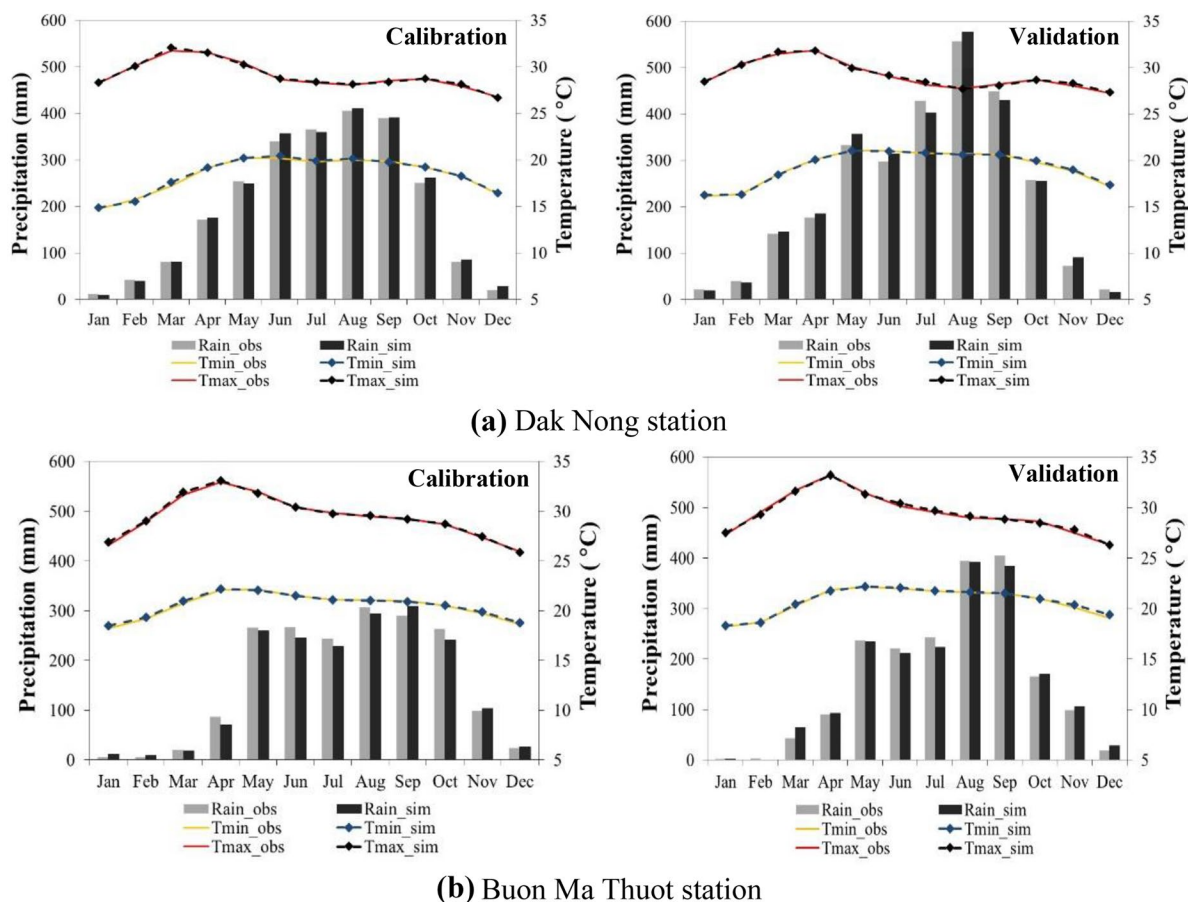


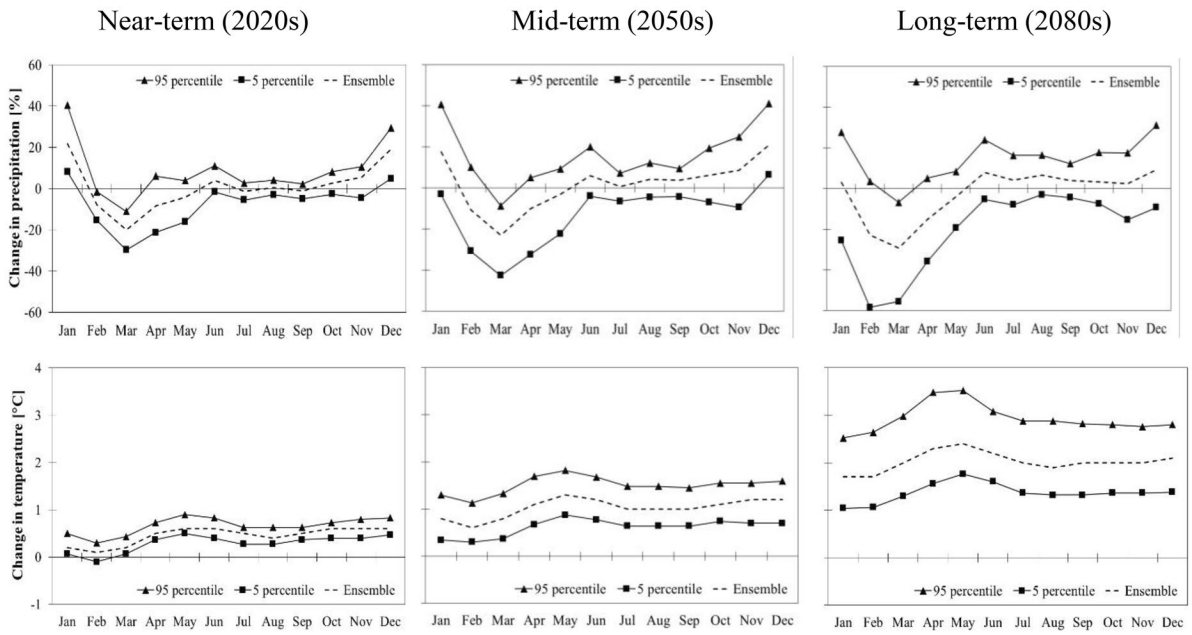
**Fig. 4** Comparison plots of observed and LARS-WG simulated averaged monthly weather data at **a** the Dak Nong station and **b** the Buon Ma Thuot station for the calibration (1981–1995) and validation (1996–2005) periods

### Joint impacts of CC and LUCC on hydrology

To explore the joint impacts of CC and LUCC, the streamflow and hydrological components under the combination of the land use/cover characteristics in 2050 and ensemble mean changes in climate for the three future periods (2020s, 2050s, and 2080s) are compared to those in the reference period (the land use/cover map in 1997 and climate in the 1981–2005 period). Figure 9 and Table 8 present changes in hydrological processes under the joint impacts of CC and LUCC.

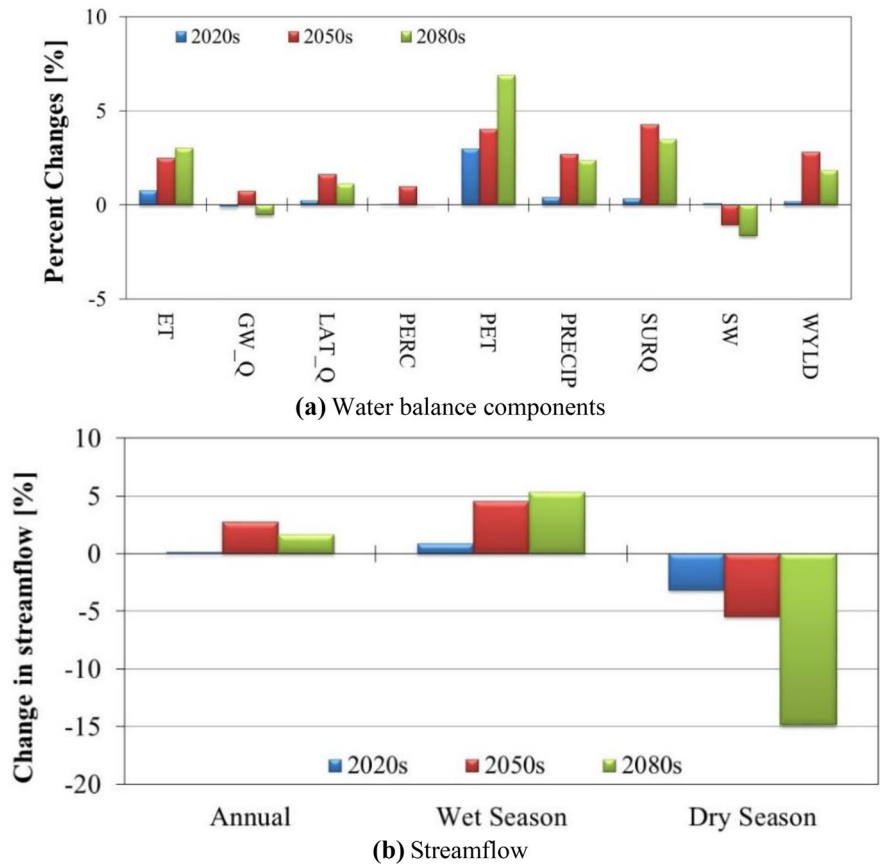
The combination of CC and LUCC increases streamflow and hydrological components except for GW\_Q and PERC. When the changes in hydrological processes under the separate impacts of CC and LUCC are in the same direction, these changes will intensify under the

combined impact of CC and LUCC. In contrast, when the directions of the changes under the impacts of CC alone and LUCC alone are opposite, these changes will reduce under the coupled impact of CC and LUCC. The ET, LAT\_Q, PET, SURQ, and WYLD are projected to increase from 1.0 to 3.1%, 0.1 to 1.4%, 1.3 to 6.9%, 1.6 to 5.6%, and 0.1 to 1.8%, respectively. The other hydrological components, including GW\_Q, PERC, and SW, reduce by 1.5 to 2.7%, 1.1 to 2.1%, and 0.1 to 1.8%, respectively. On the whole, GW\_Q and PERC are more strongly affected by LUCC than CC, and ET, PET, SW, and WYLD are more strongly affected by CC than LUCC. In fact, GW\_Q and PERC are related to water movement within the soil layers, which is strongly affected by land use/cover types. In addition, ET and PET are strongly affected by temperature and SW and WYLD are mainly determined by evaporation and precipitation.



**Fig. 5** Monthly changes in precipitation and temperature during the 2020s, 2050s, and 2080s

**Fig. 6** Percent changes in hydrological processes under the CC impact. **a** Water balance components. **b** Streamflow



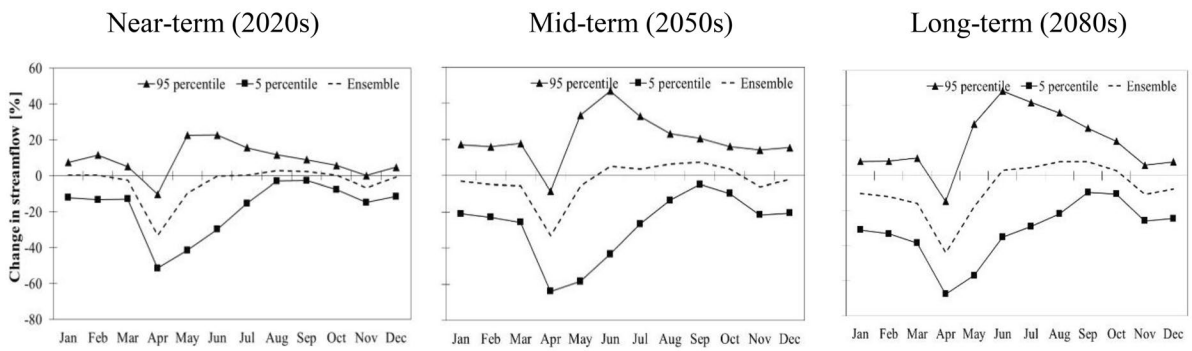


**Fig. 7** Monthly changes in streamflow during the 2020s, 2050s, and 2080s

For example, high temperature increases evaporation, which then reduces SW. In addition, high precipitation directly leads to increases in SW and WYLD (Tan et al., 2015).

Considering the streamflow changes under the joint impact of CC and LUCC, the annual streamflow increases slightly from 0.2 to 2.8%. Seasonally, increases in the wet-seasonal streamflow (by 0.5 to

**Fig. 8** Percent changes in hydrological processes under the LUCC impact

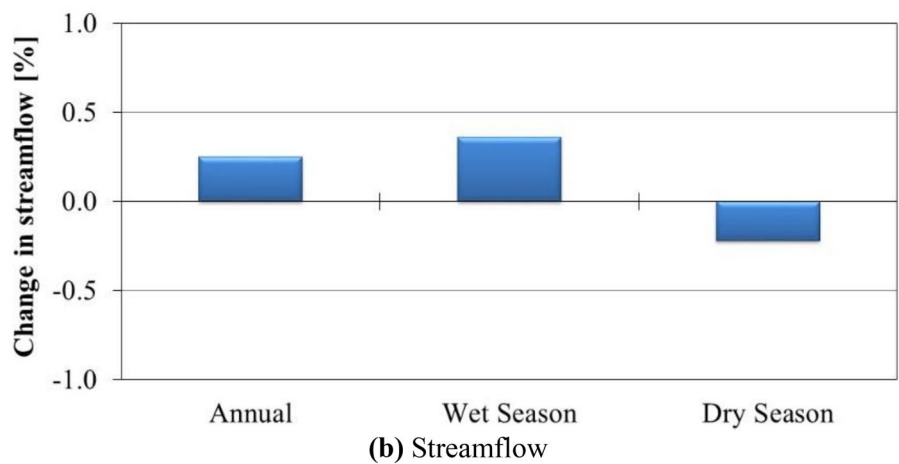
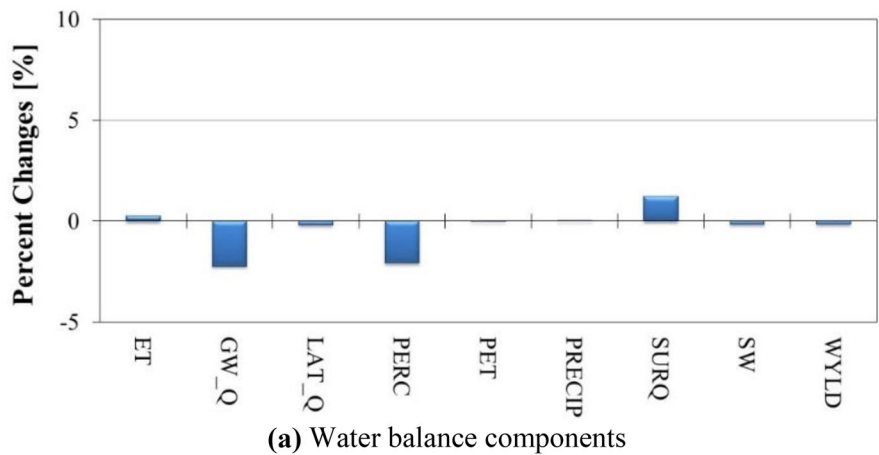
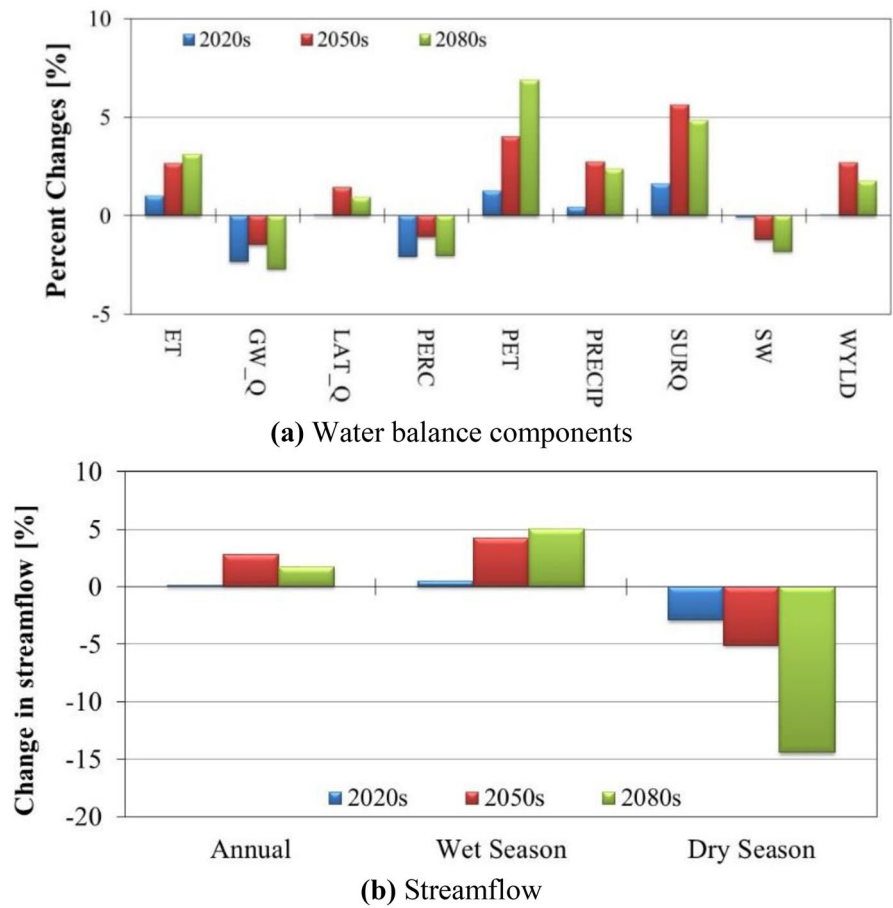


**Fig. 9** Percent changes in hydrological processes under the combined impact of CC and LUCC



5.1%) and reductions in the dry-seasonal streamflow are predicted to occur in the future. In general, the streamflow will have stronger responses to CC than to LUCC. Actually, it is easy to recognize that the magnitude of change in streamflow under the CC impact

seems to be smaller than that under the LUCC impact as described in Sects. 4.3 and 4.4. This can be attributed to the reduction in forest land mainly happens in the uppermost area of the basin (Fig. 2).

**Table 8** Relative changes in water balance components and streamflow under the separate and combined impacts of future CC and LUCC compared to the baseline period

	Only CC			Only LUCC	Combined CC and LUCC		
	2020s	2050s	2080s		2020s	2050s	2080s
ET	0.8%	2.5%	3.0%	0.3%	1.0%	2.7%	3.1%
GW_Q	-0.1%	0.7%	-0.5%	-2.2%	-2.3%	-1.5%	-2.7%
LAT_Q	0.2%	1.6%	1.1%	-0.2%	0.1%	1.4%	0.9%
PERC	0.0%	1.0%	0.0%	-2.1%	-2.1%	-1.1%	-2.0%
PET	1.3%	4.0%	6.9%	0.0%	1.3%	4.0%	6.9%
PRCP	0.4%	2.7%	2.2%	-	0.4%	2.7%	2.2%
SURQ	0.4%	4.3%	3.5%	1.2%	1.6%	5.6%	4.8%
SW	0.1%	-1.1%	-1.7%	-0.2%	-0.1%	-1.2%	-1.8%
WYLD	0.2%	2.8%	1.8%	-0.1%	0.0%	2.7%	1.8%
Streamflow	0.1%	2.7%	1.7%	0.3%	0.2%	2.8%	1.9%

## Discussion

This study found that streamflow of the SRB would increase under the CC impact. This result agrees with other studies carried out in the Vietnam's Central Highland (Huyen et al., 2017; Kawasaki et al., 2010; Raghavan et al., 2014). Specifically, Kawasaki et al. (2010) reported a 3 to 6% increase in streamflow, Raghavan et al. (2014) showed a 40% increase in annual streamflow and Huyen et al. (2017) indicated a 1.2 to 11.1% reduction in streamflow using the A1B scenario and a 1.4 to 2.4% increase in streamflow using the A2 scenario. These differences here are understandable because the future climate scenarios in those studies were generated based on the assumptions or output from a GCM. In the view of LUCC, the streamflow is projected to have upward trend in the future. The hydrological effects of LUCC in different areas of Vietnam have been examined in some studies. As an example, Khoi and Suetsugi (2014) reported that a 16.3% reduction in forestland causes a 0.2 to 0.4% increase in streamflow in the Be River Catchment in South Vietnam. Additionally, Ngo et al. (2015) reported that the transformation of forestland to cropland and urban is a cause of an 88% increase in annual runoff in the Da River Catchment in Northwest Vietnam. On the whole, the change in streamflow ascribed to the LUCC in the SRB concurs with the findings of Khoi and Suetsugi (2014) and Ngo et al. (2015). Under the combined impacts of CC and LUCC, the findings of this work are indistinguishable to the conclusions of studies discussed by Khoi and Suetsugi (2014), Khoi and Thom (2015b), and Tan et al. (2015).

In this work, climate change scenarios were developed using an average ensemble of GCM outputs, which can partly reduce the uncertainty in climate change scenarios. The LARS-WG downscaling method was adopted to build climate change scenarios for the SRB. Among the statistical downscaling tools, only LARS-WG has a fairly comprehensive database that embeds over GCM outputs used in IPCC-AR5. The database is expected to help hydrological impact studies in managing the uncertainty in GCM outputs (Qin & Lu, 2014). The LUCC scenario in this work inherited from the study of Ty et al. (2012) is relatively simple, and it was built based on trends of historical changes in land use/cover types, with the driving factor of population growth. Other driving factors on LUCC (e.g., future

climate, GDP, socio-economic development, and environmental conservation) were not considered in developing the LUCC scenario. In addition, the LUCC scenario did not consider specific assumptions of climate change scenarios. In future study, LUCC scenarios will be generated by considering these shortcomings. Moreover, the future land use/cover in different time slices should be considered to improve the hydrological impact projections.

A general study on the uncertainty linked to GCM outputs, GHG emission scenarios, downscaling methods, land use/cover change scenarios, and hydrological models is necessary to determine the main sources of uncertainty. In this work, we used reliable data and applied a standard modelling method designed to significantly reduce this uncertainty.

## Conclusion

This study assesses the individual and joint impacts of future CC and LUCC on the regional hydrological processes in the SRB. The calibrated and validated SWAT model was used for examining the hydrological impacts of environmental changes, including CC and LUCC.

CC analysis displays increases in future temperature and precipitation with respect to the reference period. Hydrological analysis under the CC impact shows upwards trends in streamflow and hydrological components except for groundwater discharge and soil water content. Additionally, the CC impact will exacerbate serious problems related to water shortages in the dry season. LUCC causes increases in streamflow and surface runoff and decreases in groundwater discharge, and they reduce the amount of water percolating out of the root zone. These changes can be explained by deforestation and intensified agricultural expansion. In addition, these changes raise concerns regarding water shortage in the dry season. Analysis of the coupled impact of CC and LUCC indicates that streamflow and hydrological components (except for groundwater discharge and water percolation amounts) are more sensitive to CC than LUCC. Moreover, it is highlighted that the water scarcity in the dry-seasonal months may occur in the future.

This work could be useful for managing and planning freshwater resources in this region and for developing adaptation and mitigation strategies in CC and LUCC.



**Acknowledgements** This research is funded by Vietnam National Foundation for Science and Technology Development (NAFOSTED) under grant number “105.06-2019.20.” The authors also would like to thank the anonymous reviewer for their valuable and constructive comments to improve our manuscript.

**Author contribution** Pham Thi Thao Nhi: methodology; software; formal analysis; writing—review and editing. Dao Nguyen Khoi: conceptualization; methodology; formal analysis; funding acquisition; writing—review and editing; Nguyen Thi Thuy Trang: software; formal analysis; writing—review and editing; Tran Van Ty: software; formal analysis; writing—review and editing; Shibo Fang: methodology, formal analysis, writing—review and editing.

**Data availability** Not applicable.

**Declarations**

**Ethics approval** Not applicable.

**Consent to participate** Not applicable.

**Consent for publication** Not applicable.

**Competing interests** The authors declare no competing interests.

**References**

Abbaspour, K. C. (2015). *SWAT-CUP: SWAT Calibration and Uncertainty Programs - a user manual*. Eawag: Swiss Federal Institute of Aquatic Science and Technology.

Abera, W., Tamene, L., Abegaz, A., & Solomon, D. (2019). Understanding climate and land surface changes impact on water resources using Budyko framework and remote sensing data in Ethiopia. *Journal of Arid Environments*, 167, 56–64. <https://doi.org/10.1016/j.jaridenv.2019.04.017>

Agarwal, A., Babel, M. S., & Maskey, S. (2014). Analysis of future precipitation in the Koshi river basin. *Nepal. Journal of Hydrology*, 513, 422–434. <https://doi.org/10.1016/j.jhydrol.2014.03.047>

Allani, M., Mezzi, R., Zouabi, A., Béji, R., Joumade-Mansouri, F., Hamza, M. E., & Sahli, A. (2020). Impact of future climate change on water supply and irrigation demand in a small mediterranean catchment. Case study: Nebhana dam system, Tunisia. *Journal of Water and Climate Change*, 11(4), 1724–1747. <https://doi.org/10.2166/wcc.2019.131>

Azmat, M., Qamar, M. U., Huggel, C., & Hussain, E. (2018). Future climate and cryosphere impacts on the hydrology of a scarcely gauged catchment on the Jhelum river basin, Northern Pakistan. *Science of the Total Environment*, 639, 961–976. <https://doi.org/10.1016/j.scitotenv.2018.05.206>

Bao, Z., Zhang, J., Wang, G., Chen, Q., Guan, T., Yan, X., et al. (2019). The impact of climate variability and land use/cover change on the water balance in the Middle Yellow

River Basin. *China. Journal of Hydrology*, 577, 123942. <https://doi.org/10.1016/j.jhydrol.2019.123942>

Chen, H., Guo, J., Zhang, Z., & Xu, C.-Y. (2013). Prediction of temperature and precipitation in Sudan and South Sudan by using LARS-WG in future. *Theoretical and Applied Climatology*, 113(3–4), 363–375. <https://doi.org/10.1007/s00704-012-0793-9>

Chen, Q., Chen, H., Zhang, J., Hou, Y., Shen, M., Chen, J., & Xu, C. (2020). Impacts of climate change and LULC change on runoff in the Jinsha River Basin. *Journal of Geographical Sciences*, 30(1), 85–102. <https://doi.org/10.1007/s11442-020-1716-9>

Cheng, Z., & Yu, B. (2019). Effect of land clearing and climate variability on streamflow for two large basins in Central Queensland. *Australia. Journal of Hydrology*, 578, 124041. <https://doi.org/10.1016/j.jhydrol.2019.124041>

El-Khoury, A., Seidou, O., Lapen, D. R., Que, Z., Mohammadian, M., Sunohara, M., & Bahram, D. (2015). Combined impacts of future climate and land use changes on discharge, nitrogen and phosphorus loads for a Canadian river basin. *Journal of Environmental Management*, 151, 76–86. <https://doi.org/10.1016/j.jenvman.2014.12.012>

Fan, M., & Shibata, H. (2015). Simulation of watershed hydrology and stream water quality under land use and climate change scenarios in Teshio River watershed, northern Japan. *Ecological Indicators*, 50, 79–89. <https://doi.org/10.1016/j.ecolind.2014.11.003>

Han, Z., Long, D., Fang, Y., Hou, A., & Hong, Y. (2019). Impacts of climate change and human activities on the flow regime of the dammed Lancang River in Southwest China. *Journal of Hydrology*, 570, 96–105. <https://doi.org/10.1016/j.jhydrol.2018.12.048>

Hassan, Z., Shamsudin, S., & Harun, S. (2014). Application of SDSM and LARS-WG for simulating and downscaling of rainfall and temperature. *Theoretical and Applied Climatology*, 116(1–2), 243–257. <https://doi.org/10.1007/s00704-013-0951-8>

Hoan, N. X., Khoi, D. N., & Nhi, P. T. T. (2020). Uncertainty assessment of streamflow projection under the impact of climate change in the Lower Mekong Basin: A case study of the Srepok River Basin. *Vietnam. Water and Environment Journal*, 34(1), 131–142. <https://doi.org/10.1111/wej.12447>

Hung, C.-L.J., James, L. A., Carbone, G. J., & Williams, J. M. (2020). Impacts of combined land-use and climate change on streamflow in two nested catchments in the Southeastern United States. *Ecological Engineering*, 143, 105665. <https://doi.org/10.1016/j.ecoleng.2019.105665>

Huyen, N. T., Tu, L. H., Tram, V. N. Q., Minh, D. N., Liem, N. D., & Loi, N. K. (2017). Assessing the impacts of climate change on water resources in the Srepok watershed, Central Highland of Vietnam. *Journal of Water and Climate Change*, 8(3), 524–534. <https://doi.org/10.2166/wcc.2017.135>

IPCC. (2013). *The Physical Science Basis: Contribution of working group I to the fifth assessment report of Intergovernmental Panel on climate change*. Cambridge University Press.

Kavwenje, S., Zhao, L., Chen, L., & Chaima, E. (2021). Projected temperature and precipitation changes using the LARS-WG statistical downscaling model in the Shire River Basin, Malawi. *International Journal of Climatology*, joc.7250. <https://doi.org/10.1002/joc.7250>

- Kawasaki, A., Takamatsu, M., He, J., Rogers, P., & Herath, S. (2010). An integrated approach to evaluate potential impact of precipitation and land-use change on streamflow in the Srepok River Basin. *Theory and Application of GIS*, 18(2), 9–20.
- Khoi, D. N., & Suetsugi, T. (2012). Uncertainty in climate change impacts on streamflow in Be River Catchment. *Vietnam. Water and Environment Journal*, 26(4), 530–539. <https://doi.org/10.1111/j.1747-6593.2012.00314.x>
- Khoi, D. N., & Suetsugi, T. (2014). The responses of hydrological processes and sediment yield to land-use and climate change in the Be River Catchment. *Vietnam. Hydrological Processes*, 28(3), 640–652. <https://doi.org/10.1002/hyp.9620>
- Khoi, D. N., & Thom, V. T. (2015a). Impacts of climate variability and land-use change on hydrology in the period 1981–2009 in the central highlands of vietnam. *Global Nest Journal*, 17(4), 870–881.
- Khoi, D. N., & Thom, V. T. (2015b). Parameter uncertainty analysis for simulating streamflow in a river catchment of Vietnam. *Global Ecology and Conservation*, 4, 538–548. <https://doi.org/10.1016/j.gecco.2015.10.007>
- Khoi, D. N., Thom, V. T., Quang, C. N. X., & Phi, H. L. (2017). Parameter uncertainty analysis for simulating streamflow in the upper Dong Nai river basin. *Houille Blanche*, 1, 14–23. <https://doi.org/10.1051/lhb/2017003>
- Knutti, R., Abramowitz, G., Collins, M., Eyring, V., Gleckler, P. J., Hewitson, B., & Mearns, L. (2010). *Good Practice Guidance Paper on Assessing and Combining Multi Model Climate Projections*. Bern, Switzerland.
- Ma, X., Xu, J., Luo, Y., Prasad Aggarwal, S., & Li, J. (2009). Response of hydrological processes to land-cover and climate changes in Kejie watershed, south-west China. *Hydrological Processes*, 23(8), 1179–1191. <https://doi.org/10.1002/hyp.7233>
- Meyfroidt, P., Vu, T. P., & Hoang, V. A. (2013). Trajectories of deforestation, coffee expansion and displacement of shifting cultivation in the Central Highlands of Vietnam. *Global Environmental Change*, 23(5), 1187–1198. <https://doi.org/10.1016/j.gloenvcha.2013.04.005>
- Moriassi, D. N., Gitau, M. W., Pai, N., & Daggupati, P. (2015). Hydrologic and Water quality models: performance measures and evaluation criteria. *Transactions of the ASABE*, 58(6), 1763–1785. <https://doi.org/10.13031/trans.58.10715>
- Napoli, M., Massetti, L., & Orlandini, S. (2017). Hydrological response to land use and climate changes in a rural hilly basin in Italy. *CATENA*, 157, 1–11. <https://doi.org/10.1016/j.catena.2017.05.002>
- Neitsch, A. L., Arnold, J. G., Kiniry, J. R., Williams, J. R., Neitsch, S., Arnold, J. G., et al. (2011). *Soil and Water Assessment Tool Theoretical Documentation Version 2009*. Texas Water Resources Institute. Texas A&M University.
- Ngo, T. S., Nguyen, D. B., & Rajendra, P. S. (2015). Effect of land use change on runoff and sediment yield in Da River Basin of Hoa Binh province, Northwest Vietnam. *Journal of Mountain Science*, 12(4), 1051–1064. <https://doi.org/10.1007/s11629-013-2925-9>
- Osei, M. A., Amekudzi, L. K., Wemegah, D. D., Preko, K., Gyawu, E. S., & Obiri-Danso, K. (2019). The impact of climate and land-use changes on the hydrological processes of Owabi catchment from SWAT analysis. *Journal of Hydrology: Regional Studies*, 25, 100620. <https://doi.org/10.1016/j.ejrh.2019.100620>
- Qin, X. S., & Lu, Y. (2014). Study of climate change impact on flood frequencies: A combined weather generator and hydrological modeling approach. *Journal of Hydrometeorology*, 15(3), 1205–1219. <https://doi.org/10.1175/JHM-D-13-0126.1>
- Raghavan, S. V., Tue, V. M., & Shie-Yui, L. (2014). Impact of climate change on future stream flow in the Dakbla river basin. *Journal of Hydroinformatics*, 16(1), 231–244. <https://doi.org/10.21666/hydro.2013.165>
- Semenov, M., & Stratonovitch, P. (2010). Use of multi-model ensembles from global climate models for assessment of climate change impacts. *Climate Research*, 41, 1–14. <https://doi.org/10.3354/cr00836>
- Setyorini, A., Khare, D., & Pingale, S. M. (2017). Simulating the impact of land use/land cover change and climate variability on watershed hydrology in the Upper Brantas basin. *Indonesia. Applied Geomatics*, 9(3), 191–204. <https://doi.org/10.1007/s12518-017-0193-z>
- Shrestha, S., Bhatta, B., Shrestha, M., & Shrestha, P. K. (2018). Integrated assessment of the climate and landuse change impact on hydrology and water quality in the Songkhram River Basin, Thailand. *Science of the Total Environment*, 643, 1610–1622. <https://doi.org/10.1016/j.scitotenv.2018.06.306>
- Tan, M. L., Ibrahim, A. L., Yusop, Z., Duan, Z., & Ling, L. (2015). Impacts of land-use and climate variability on hydrological components in the Johor River basin. *Malaysia. Hydrological Sciences Journal*. <https://doi.org/10.1080/02626667.2014.967246>
- Tram, V. N. Q., Liem, N. D., & Loi, N. K. (2019). Simulating surface flow and baseflow in Poko catchment, Kon Tum province. *Vietnam. Journal of Water and Climate Change*, 10(3), 494–503. <https://doi.org/10.2166/wcc.2018.185>
- Trang, N. T. T., Shrestha, S., Shrestha, M., Datta, A., & Kawasaki, A. (2017). Evaluating the impacts of climate and land-use change on the hydrology and nutrient yield in a transboundary river basin: A case study in the 3S River Basin (Sekong, Sesan, and Srepok). *Science of the Total Environment*, 576, 586–598. <https://doi.org/10.1016/j.scitotenv.2016.10.138>
- Ty, T. V., Sunada, K., Ichikawa, Y., & Oishi, S. (2012). Scenario-based impact assessment of land use/cover and climate changes on water resources and demand: A case study in the Srepok River Basin, Vietnam—Cambodia. *Water Resources Management*, 26(5), 1387–1407. <https://doi.org/10.1007/s11269-011-9964-1>
- Wilby, R. L., & Dawson, C. W. (2007). *SDSM 4.2 – A decision support tool for assessment of regional climate change impacts*.
- Woldesenbet, T. A., Elagib, N. A., Ribbe, L., & Heinrich, J. (2017). Hydrological responses to land use/cover changes in the source region of the Upper Blue Nile Basin, Ethiopia. *Science of the Total Environment*, 575, 724–741. <https://doi.org/10.1016/j.scitotenv.2016.09.124>
- Zhang, L., Nan, Z., Xu, Y., & Li, S. (2016). Hydrological impacts of land use change and climate variability in the Headwater Region of the Heihe River Basin. *Northwest China. Plos One*, 11(6), e0158394. <https://doi.org/10.1371/journal.pone.0158394>

**Publisher's Note** Springer Nature remains neutral with regard to jurisdictional claims in published maps and institutional affiliations.